01 Jul 2011

Electric Breakdown of Longitudinally Shocked $Pb(Zr_{0.52}Ti_{0.48})O_3$ Ceramics

S. I. Shkuratov

E. F. Talantsev

Jason Baird
Missouri University of Science and Technology, jbaird@mst.edu

Recommended Citation

S. I. Shkuratov et al., "Electric Breakdown of Longitudinally Shocked $Pb(Zr_{0.52}Ti_{0.48})O_3$ Ceramics," *Journal of Applied Physics*, vol. 110, American Institute of Physics (AIP), Jul 2011.
The definitive version is available at https://doi.org/10.1063/1.3609074

Electric breakdown of longitudinally shocked $Pb(Zr_{0.52}Ti_{0.48})O_3$ ceramics

Sergey I. Shkuratov,[1,a] Evgueni F. Talantsev,[2] and Jason Baird[1,3]
[1]*Loki Incorporated, Rolla, Missouri 65409, USA*
[2]*Pulsed Power LLC, Lubbock, Texas 79416, USA*
[3]*Department of Mining and Nuclear Engineering, Missouri University of Science and Technology, Rolla, Missouri 65409-0450, USA*

(Received 2 May 2011; accepted 9 June 2011; published online 27 July 2011)

Electric breakdown of longitudinally-shock-compressed $Pb(Zr_{0.52}Ti_{0.48})O_3$ (PZT 52/48) ferroelectric ceramics was experimentally investigated. It was found that a dependence of breakdown field strength, E_g, of shocked ferroelectrics on the thickness of the element, d, ranging from 0.65 to 6.5 mm is described by the $E_g(d) = \gamma \cdot d^{-w}$ law that describes the breakdown of dielectrics at ambient conditions. It follows from the experimental results that the tunnel effect is a dominant mechanism of injection of prime electrons in the shocked ferroelectric elements. It was demonstrated that electric breakdown causes significant energy losses in miniature autonomous generators based on shock depolarization of poled ferroelectric elements. © *2011 American Institute of Physics*. [doi:10.1063/1.3609074]

I. INTRODUCTION

Extensive studies of ferroelectrics under shock wave compression have been performed since the end of the 1950s and continue until the present time (see Ref. 1 and references therein). One of the effects associated with the shock-wave compression of poled ferroelectrics is the generation of a high electric field within the ferroelectric elements due to the shock depolarization.[2] Before the shock compression, the electric field in the ferroelectric element is equal to zero because of compensation by the surface charge (the bonded charge) of the polarization of the element, $\boldsymbol{P}_0$, obtained during the poling procedure. Shock depolarization releases the bonded charge at the electrodes, and correspondingly, a high electric potential and a high electric field appear across the element. Miniature autonomous electrical systems called shock wave ferroelectric generators[3] (FEGs) utilize the ability of shocked ferroelectrics to generate high voltage. The FEGs (with total volume less than 100 cm^3 and based on shock depolarization of $Pb(Zr_{0.52}Ti_{0.48})O_3$ poled ferroelectrics) demonstrate reliable operation and are capable of producing high voltages.[3–5] These generators were successfully used for charging capacitor banks and as prime power stages for 90-kV nanosecond pulsed power systems, and are regarded as a new class of miniature autonomous high-voltage pulsed power sources.[1,3–8]

The high electric voltage produced by the FEGs can cause electric breakdown in the shocked ferroelectric elements. Electric breakdown in shocked piezoelectric and ferroelectric materials has been widely discussed since the 1960s.[9] It was experimentally demonstrated in Ref. 10 that the mechanism of the breakdown of non-shocked (ambient condition) ferroelectric samples poled to full remnant polarization is similar to that of conventional dielectric materials.[11–15] It was assumed in Ref. 16 that breakdown in shocked ferroelectric samples could be predicted from ambient and quasi-static loading data. A series of experimental and theoretical studies of the electric breakdown of shock-compressed $Pb(Zr_{0.64}Ti_{0.36})O_3$ (PZT 65/35) ferroelectrics poled to different polarization levels (Q_0 varied from 3 to 30 $\mu C/cm^2$) were performed in Ref. 16. These studies revealed the complex relationship between the breakdown field, polarization of the samples, and shock pressure (P_{SW}, which varied from 0.3 to 2.3 GPa). The breakdown mechanism in shock-compressed ferroelectrics is still not a completely understood phenomenon.[1,10,16]

In this paper we conducted systematic studies of the operation of miniature FEGs based on longitudinal (the shock wave front propagated along the polarization vector $\boldsymbol{P}_0$) shock depolarization of PZT 52/48 poled ferroelectrics along with measurements of the quasi-static thermal depolarization of ferroelectric samples. Our experimental results showed that the ferroelectric elements shocked within the FEGs operating with a low-resistance load were able to release an amount of electric charge almost equal to that stored in the elements due to the poling procedure. When we operated FEGs with a high resistance load, a significant electric charge loss with its attendant significant energy loss occurred in the generators. These losses are related to the internal breakdown within the ferroelectric elements. Analysis of these experimental data allowed us to obtain a relatively simple relationship for a prediction of breakdown field in shocked ferroelectric elements and to identify the basic physics of breakdown mechanisms in shock-compressed ferroelectric materials.

II. MATERIALS AND EXPERIMENTAL TECHNIQUES

PZT 52/48 (EC-64) ceramic disks supplied by ITT Corporation were used in all experiments described in this paper. The sizes of the PZT 52/48 elements studied are in Table I. The manufacturer deposited 17 ± 2 μm-thick silver contact plates (electrodes) on both faces of each PZT 52/48 disk. Each sample was poled to its remnant polarization by the

[a]Author to whom correspondence should be addressed. Electronic mail: shkuratov@lokiconsult.com.

TABLE I. Sizes and polarization rate of studied $Pb(Zr_{0.52}Ti_{0.48})O_3$ ceramic disk elements.

FEG designation	Case 1	Case 2	Case 3	Case 4	Case 5
Element diameter, D (mm)	26.2 ± 0.5	27.0 ± 0.5	25.0 ± 0.3	25.0 ± 0.3	25.0 ± 0.3
Element thickness, d (mm)	0.65 ± 0.04	2.1 ± 0.1	2.5 ± 0.1	5.1 ± 0.1	6.5 ± 0.1
Thermal depolarization charge density, $Q_{dep\ therm}$ ($\mu C/cm^2$)	27.9 ± 1.8	27.8 ± 1.5	27.4 ± 1.7	27.9 ± 1.6	27.6 ± 1.8
Shock pressure depolarization charge density, $Q_{dep\ sw}$ ($\mu C/cm^2$)	29.7 ± 2.4	27.5 ± 2.2	27.1 ± 2.3	25.7 ± 2.2	22.3 ± 2.4
Calculated electric field strength, E_c (kV/mm)	29.4	27.3	26.9	25.5	22.1
Experimental electric field strength, E_g (kV/mm)	5.5 ± 0.5	3.8 ± 0.4	3.7 ± 0.3	3.2 ± 0.3	3.1 ± 0.3

manufacturer. The properties of PZT 52/48 (EC-64) are in Table II.

For measurements of actual polarization of studied PZT 52/48 samples, we used a quasi-static thermal depolarization procedure. For the procedure, we placed a ferroelectric sample in a beaker filled with ultra-fine sand (a thermal bath) in an automatically controlled Thermolyne 47 900 furnace. The controlling K-type thermocouple was connected to a Sper Scientific thermometer (model 800 005). During the procedure, we monitored the current in the ferroelectric samples with a Keithley 2400 pico-ampere meter. The heating rate (0.9 K/min) was the same for the entire temperature range (295 through 650 K), and for all samples studied.

Explosive experiments were conducted in the facilities of the Energetic Materials Research Laboratory of the Missouri University of Science and Technology, Rolla, MO. We used explosively driven FEGs (Ref. 3) that provide highly reproducible shock wave profiles and shock pressure $P_{SW} = 1.5 \pm 0.1$ GPa in the investigated samples.[8] A schematic diagram of the FEG design we used is in Fig. 1. The FEG contained a ferroelectric element, a detonation chamber with high explosive (HE) charge, and metallic impactor (flyer plate). The overall dimensions of the FEGs used in the experiments did not exceed 50 mm. The operation of the FEG was as following. The flyer plate, accelerated to high velocity by the detonation of the HE charge, impacted the ferroelectric body so that the shock wave traveled in a direction parallel to the vector $\boldsymbol{P}_0$ (Fig. 1). When a shock wave depolarizes a ferroelectric disk, a pulsed electric potential (an electromotive force, or EMF) appears on the metallic electrodes of the ferroelectric element.

We performed a series of experiments to measure an amount of electric charge released by longitudinally shocked elements of the FEGs. A schematic diagram of the setup for shock depolarization experiments is in Fig. 2(a). To provide accurate measurement of the electric charge released due to the shock depolarization, the load of the FEG was a low-resistance ($R_L(100\ \text{kHz}) = 0.5\ \Omega$) and low-inductance ($L_L(100\ \text{kHz}) = 0.98\ \mu\text{H}$) copper loop.

We used a Tektronix 6015 A high voltage probe (resistance $R_L = 10^8\ \Omega$) as the load in the experiments with FEGs operating in the high voltage mode [Fig. 2(b)]. The pulsed signals were recorded with an HP Agilent 54 845 A oscilloscope (bandwidth 1.5 GHz, 8 GSa/s).

TABLE II. Physical properties of the PZT 52/48 (EC-64) ferroelectric ceramics.

Property	Value
Density (10^3 kg/m^3)	7.5
Young's modulus (10^{10} N/m^2)	7.8
Curie temperature (°C)	320
Mechanical Q for a thin disc	400
Dielectric constant at 1 kHz (poled)	1300
Dielectric constant at 1 kHz (unpoled)	1140
Dielectric constant aging rate (% changes per time decade)	−4.2
Piezoelectric constant d_{33} (10^{-12} m/V)	295
Piezoelectric constant g_{33} (10^{-3} m/N)	25.0
Elastic constant s_{11}^E (10^{-12} m^2/N)	12.8

III. RESULTS AND DISCUSSIONS

The amount of electric charge released at the electrodes of its shock-compressed ferroelectric element in the course of explosive operation of the FEG is one of the main parameters that determine the ability of the FEG to produce high voltage. To measure the electric charge generated by shocked PZT 52/48 elements and to estimate the degree of their depolarization, we utilized the approach that was developed in Ref. 8, i.e., measurements of depolarization of ferroelectric samples by means of two techniques, explosive shock compression and quasi-static thermal heating. We extended the data obtained in Ref. 8 with measurements of elements studied in this paper. The electric charge released by PZT 52/48 samples, Q_{dep}, was obtained by integrating the current, $I(t)$, flowing in the circuit of the explosively driven FEG [Fig. 2(a)] or in the thermal depolarization circuit:

$$Q_{dep} = \int_0^\infty I(t) \cdot dt. \tag{1}$$

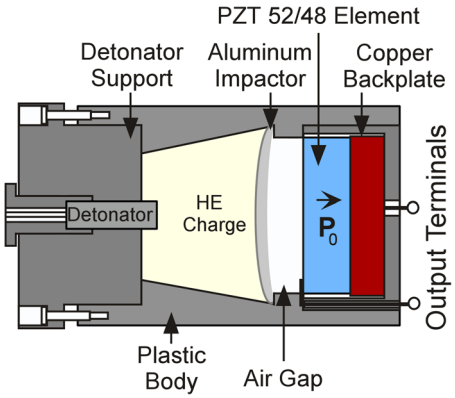

FIG. 1. (Color online) Schematic diagram of the longitudinal FEG.

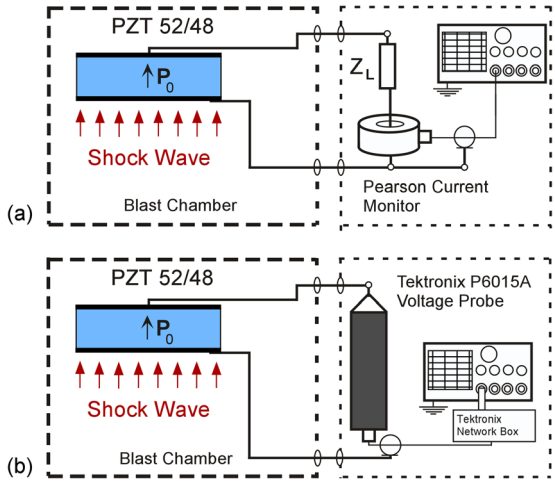

FIG. 2. (Color online) Schematic diagrams of the experimental setup (a) for investigation of longitudinal shock wave depolarization of the PZT 52/48 ferroelectrics and (b) for investigations of operation of the FEGs with a high resistance load.

Table I and Fig. 3 contain summaries of the results of our shock and thermal depolarization experiments. It follows from the experimental results that practically all bonded electric charges initially stored in the PZT 52/48 elements having thickness from 0.65 to 2.5 mm were released due to longitudinal shock compression in the load circuit of the FEGs. For samples with thickness 5.1 and 6.5 mm, the shock depolarization charge density, $Q_{dep\ sw}$, is lower than that obtained in thermal depolarization experiments, $Q_{dep\ therm}$ (Fig. 3). This effect can be explained by the shock wave splitting phenomena observed earlier.[17] It was shown in Ref. 17 that a longitudinal shock wave in PZT 52/48 splits into two shock waves, and the split shocks result in a decreased depolarization charge. An increase of the thickness of the elements up to 6.5 mm leads to an increase in shock wave travel distance and to a more significant separation of the shock waves.

The equivalent circuit of the FEG operating with a resistance load is in Fig. 4. A ferroelectric element is a capacitor. When it is connected to a high resistance load [$R_L = 10^8$

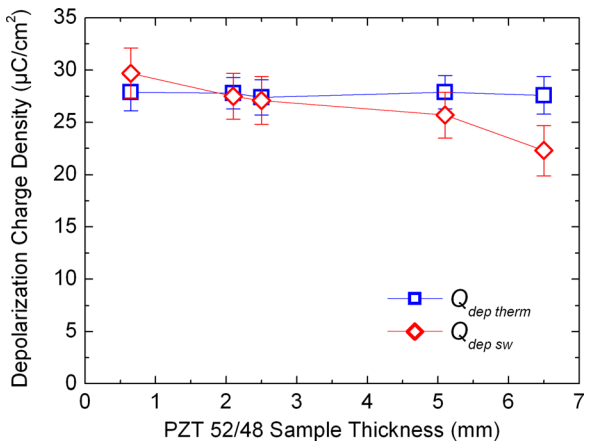

FIG. 3. (Color online) Depolarization charge density released due to the shock wave (diamonds) and thermal (squares) depolarization of PZT 52/48 elements.

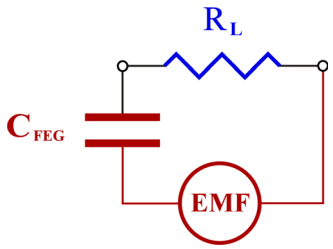

FIG. 4. (Color online) Equivalent circuit of the FEG operating with a resistance load.

Ω, Fig. 2(b)], the shock depolarization charge charges the element itself. The current passing through the load is negligible (less 10^{-3} A) and the expected electric field, E_c, within the shocked PZT element can be calculated using the following expression:

$$E_c = U_g/d = Q_{dep\,sw}/(C_{spec} \cdot d), \tag{2}$$

where U_g is the voltage generated across the shocked PZT 52/48 element, d is the element thickness, and C_{spec} is the specific capacitance of the element. The C_{spec} can be determined from the dielectric properties and geometrical dimensions of the element:

$$C_{spec} = \varepsilon \cdot \varepsilon_0/d, \tag{3}$$

where ϵ_0 is the vacuum dielectric constant and ϵ is the relative dielectric constant of the ferroelectric material. Correspondingly, Eq. (2) can be written as

$$E_c = Q_{dep\,sw}/(\varepsilon \cdot \varepsilon_0). \tag{4}$$

It follows from Eq. (4) that the electric field strength, E_c, within a shocked ferroelectric element depends on the depolarization charge density and dielectric properties of the material. We measured $Q_{dep\ sw}$ for all PZT 52/48 elements studied in this work (Fig. 3 and Table I). Accurate measurement of the relative dielectric constant of shocked ferroelectrics is an extremely difficult task. To calculate the electric field within shocked PZT 52/48 elements, we used the value of ϵ for unpoled ferroelectric ceramics provided by the manufacturer, $\epsilon = 1140$ (Table II).[14] Substitution of all parameters into Eq. (4) gives us values of E_c that vary from 22.1 to 29.4 kV/mm (Table I). Values of E_c calculated by this simple model [Eqs. (2) through (4)] are in good agreement with results of the calculations obtained with a more complicated model developed in Ref. 18.

Typical experimental waveforms of the output voltage, $U_{FEG}(t)$, produced by FEGs operating with high resistance loads [Fig. 2(b)] for Cases 1, 3, and 5 (see Table I) are in Fig. 5. The amplitude of the voltage pulse produced by the FEG for Case 1 (Fig. 5) was $U_{FEG}(t)_{\max} = 3.9$ kV with a rise time of 0.4 μs. The maximum electric field within the PZT element of the FEG for Case 1 in this experiment was $E_g = U_{FEG}(t)_{\max}/d = 6.0$ kV/mm (where d is the element thickness). The electric field averaged across the five experiments of this series was $E_g = 5.5 \pm 0.5$ kV/mm.

According to our experimental results, the amplitude of the FEG output voltage rose with increasing disk element thickness [$U_{FEG}(t)_{\max} = 8.7$ kV and 21.5 kV for Cases 3 and

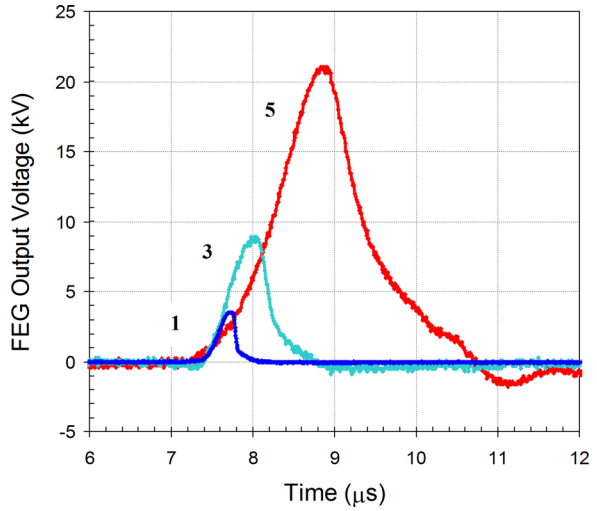

FIG. 5. (Color online) Typical waveforms of voltage pulse $U_{FEG}(t)$ produced by FEGs operating with a high resistance load for Case 1, Case 3, and Case 5.

5, respectively, in Fig. 5]. Interestingly, the maximum electric field, E_g, within each element decreased as the element thickness increased ($E_g = 3.5$ kV/mm and 3.3 kV/mm for Case 3 and Case 5, respectively, in Table I).

It follows from our experimental results (Fig. 5 and Table I) that the electric field strength across shocked PZT 52/48 elements, E_g, did not exceed 6.0 kV/mm. However, the calculated electric field, E_c, ranges from 22.1 to 29.4 kV/mm (Table I). It is evident that there are significant energy losses in shock-compressed ferroelectrics loaded with a high resistance load. A possible cause of these energy losses is an internal electric breakdown within shocked ferroelectrics.

The $U_{FEG}(t)$ waveforms for all studied cases were similar to those shown in Fig. 5: The voltage increased in an almost linear fashion to its maximum value and then rapidly decreased to zero. The increase in the $U_{FEG}(t)$ pulse from zero to its maximum value was the direct result of the depolarization of the ferroelectric element due to shock wave action. The time constant of the FEG circuit (Fig. 4) in these experiments, $\tau = R_L \cdot C_{FEG}$, was higher than 10^{-2} s. This is four orders of magnitude longer than the time for the voltage pulse to decrease (Fig. 5). It is evident that the rapid decrease of the voltage (Fig. 5) is not related to discharging the energy stored in the FEGs into the load circuit. The rapid voltage decrease could be due to a few factors: (a) Mechanical destruction of the element due to high pressure gas expansion from the HE detonation, followed by short-circuiting of the electrodes of the PZT element, (b) a significant increase of the shock-compressed ceramic material's electrical conductivity and the corresponding leakage current in the element, and (c) an internal electrical breakdown within the ceramic disk.

With regard to (a) above, the time required for mechanical destruction of the ceramics behind the shock front can be estimated as $t_{dest} = d/U_p$, where d is the thickness of the PZT disk and U_p is the particle velocity. The latter can be determined as $U_p = P_{SW}/(\rho_0 \cdot U_S)$,[19] where ρ_0 is the density of ceramics before the shock action, and U_S is the shock front velocity. In our experiments, $U_S = 3.94$ mm/μs.[8] Correspondingly $U_P = 0.05$ mm/μs, $t_{dest} = 13$ μs for Case 1 and $t_{dest} = 130$ μs for Case 5. The t_{dest} is about fifty times longer than the time of decreasing voltage in our experiments (Fig. 5), so (a) does not appear to be a factor in the rapid voltage decrease.

Similarly, for item (b) above, it follows from recent experimental studies of electrical conductivity of shock-compressed piezoelectric crystals (Ref. 20) and poled PZT ferroelectrics (Ref. 21) at $P_{SW} = 12$ GPa (nearly an order of magnitude higher than the shock pressure in the FEGs) that there is no conductivity increase in shocked PZT ceramic materials or any electric charge leakage at electric field strength up to $E = 5.3$ kV/mm.[21] So, (b) is not a factor in the rapid voltage decrease, either.

Based on the above reasoning, unless some unknown factor is at play, one can conclude that the rapid decrease of the FEG voltage (Fig. 5) is the result of internal electric breakdown in the PZT elements. Therefore, the experimentally obtained maximum output voltage, $U_{FEG}(t)_{\max}$, produced by the FEG and the maximum electric field, E_g, generated within the shocked PZT element can be considered the breakdown voltage and the breakdown field, respectively.

To analyze our experimental results, we utilized a procedure developed earlier for analysis of breakdown of dielectrics at ambient conditions.[12–15] It is generally accepted that under ambient conditions the cause of breakdown within a dielectric element is the formation of an electron avalanche, with the prime electrons being injected from the negative electrode.[13,15] Experiments verified[12–15] that at ambient conditions, the dependence of the breakdown field strength, E_g, upon the thickness of the dielectric sample, d, is described according to a law:

$$E_g(d) = \gamma \cdot d^{-w}, \tag{5}$$

where γ is a constant for the given material, and w is the coefficient that is justified by mechanisms of electric breakdown, namely the injection of electrons and electron-phonon scattering.

Table I summarizes our experimental data for the breakdown electric field, $E_g(d)$, of shocked PZT 52/48 elements. An important question presents itself: Can these data, obtained under explosive shock conditions, be described in accordance with the law [Eq. (5)] that was experimentally proven for the breakdown of dielectric materials under ambient conditions[12–15]?

In available publications (extended list of references is given in Ref. 1), we could not find any evidence that this question and this approach [Eq. (5)][12–15] have been previously applied to shocked ferroelectrics. Figure 6 presents a plot of the breakdown electric field, $\log(E_g)$, of a shocked PZT 52/48 element within a FEG as a function of element thickness, $\log(d)$. This data can be represented by a straight line, and the plot is similar to plots experimentally obtained for the breakdown electric field of dielectrics at ambient conditions.[12–15]

The slope of the curve in Fig. 6 is 0.248 ± 0.020, and this slope corresponds to the coefficient w in Eq. (5). In accordance with theoretical analysis,[13,15] a coefficient of $w = 0.25$ implies the presence of a tunnel mechanism of the

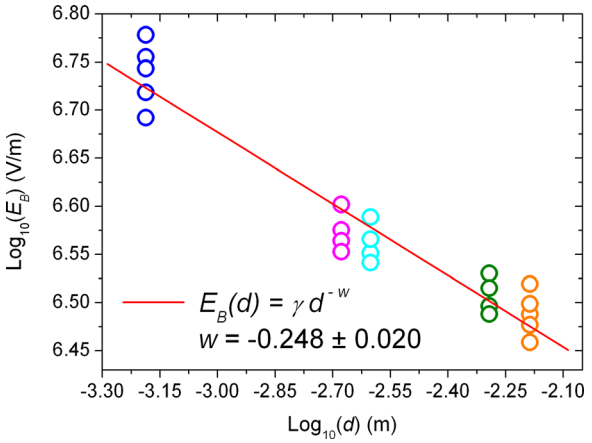

FIG. 6. (Color online) Breakdown electric field of shocked PZT 52/48 as a function of element thickness.

injection of electrons from the negative electrode into the shocked ferroelectrics, and strong electron-phonon scattering in an adiabatically compressed material. The current density, j, of the prime electrons injected into the dielectric material due to the tunnel effect is given by the following expression[13,15]:

$$j(\varphi_{eff}, E_{el}) = \frac{q_e}{16\pi^2\hbar} \cdot \frac{(q_e E_{el})^2}{\varphi_{eff}} \cdot \exp\left[-\frac{4(2m)^{\frac{1}{2}}\varphi_{eff}^{\frac{3}{2}}}{3\hbar q_e E_{el}}\right], \qquad (6)$$

where E_{el} is the electric field strength at the negative electrode, φ_{eff} is the effective height of the potential barrier at the negative electrode-dielectric interface, h is Planck's constant, and q_e and m are the charge and the effective mass of the electron, respectively.

It follows from Eq. (6) that E_{el} and φ_{eff} are the main parameters that determine the current density of the injected electrons and, correspondingly, the probability of electric breakdown of the PZT element. Apparently, a reduction of the electric field, E_{el}, through control/minimization of microprotrusions at the negative electrode surface facing the ferroelectric material and an increase of the effective height of the potential barrier, φ_{eff}, through the use of various materials in the negative electrode (it should be noted, that fundamental properties of PZT-electrode interfaces and PZT samples with electrodes made of different materials were recently studied in Ref. 22) could suppress the tunnel current density and increase the breakdown voltage of ferroelectric elements.

IV. CONCLUSIONS

Based on results reported in this paper, we conclude that internal breakdown within longitudinally shock-compressed $Pb(Zr_{0.52}Ti_{0.48})O_3$ ferroelectrics ($P_{SW} = 1.5$ GPa) is the fundamental phenomenon that affects the performance of explosive-driven shock-wave FEGs and causes significant energy losses in the devices. We have demonstrated that within shocked PZT 52/48, the dependence of the breakdown electric field, E_g, upon the element thickness, d, can be described by a law that was experimentally proved for the electric breakdown of dielectric materials at ambient conditions. Our experimental results show the tunnel effect as a dominant mechanism for the injection of prime electrons into longitudinally shock-compressed ferroelectric elements. The relationship we obtained between E_g and d allows one to predict the breakdown field in shocked ferroelectric ceramics.

[1]L. L. Altgilbers, J. Baird, B. Freeman, C. S. Lynch, and S. I. Shkuratov, *Explosive Pulsed Power* (Imperial College Press, London, 2010).
[2]F. W. Neilson, Bull. Am. Phys. Soc. **2**, 302 (1957).
[3]S. I. Shkuratov, E. F. Talantsev, L. Menon, H. Temkin, J. Baird, and L. L. Altgilbers, Rev. Sci. Instrum. **75**, 2766 (2004).
[4]S. I. Shkuratov, J. Baird, and E. F. Talantsev, Rev. Sci. Instrum. **81**, 126102 (2010).
[5]S. I. Shkuratov, J. Baird, and E. F. Talantsev, Rev. Sci. Instrum. **82**, 054701 (2011).
[6]S. I. Shkuratov, E. F. Talantsev, J. Baird, M. F. Rose, Z. Shotts, L. L. Altgilbers, and A. H. Stults, Rev. Sci. Instrum. **77**, 043904 (2006).
[7]S. I. Shkuratov, J. Baird, E. F. Talantsev, A. V. Ponomarev, L. L. Altgilbers, and A. H. Stults, IEEE Trans. Plasma Sci. **36**, 44 (2008).
[8]S. I. Shkuratov, J. Baird, V. A. Antipov, E. F. Talantsev, C. S. Lynch, L. L. Altgilbers, and A. H. Stults, IEEE Trans. Plasma Sci. **38**, 1856 (2010).
[9]R. A. Graham and W. J. Halpin, J. Appl. Phys. **39**, 5077 (1968).
[10]P. C. Lysne, J. Appl. Phys. **46**, 230 (1975).
[11]G. A. Vorob'ev, Sov. Phys. JETP **3**, 225 (1956).
[12]R. Gerson and T. C. Marshall, J. Appl. Phys. **30**, 1650 (1959).
[13]F. Forlani and N. Minnaja, Phys. Status Solidi **4**, 311 (1964).
[14]J. J. O'Dwyer, J. Appl. Phys. **39**, 4356 (1968).
[15]F. Forlani and N. Minnaja, J. Vacuum Sci. Tech. **6**, 518 (1969).
[16]P. C. Lysne and L. C. Bartel, J. Appl. Phys. **46**, 222 (1975).
[17]C. E. Reynolds and G. E. Seay, J. Appl. Phys. **33**, 2234 (1962).
[18]J. A. Mazzie, J. Appl. Phys. **48**, 1368 (1977).
[19]L. Davison, *Fundamentals of Shock Wave Propagation in Solids* (Springer, Heidelberg, 2008).
[20]V. A. Borisenok, V. A. Kruchinin, V. A. Bragunets, S. V. Borisenok, V. G. Simakov, and M. V. Zhernokletov, Combustion, Explosion, and Shock Waves **43**, 96 (2007).
[21]V. A. Bragunets, V. G. Simakov, V. A. Borisenok, S. V. Borisenok, and V. A. Kruchinin, Combustion, Explosion, and Shock Waves **46**, 231 (2010).
[22]F. Chen, R. Schafranek, A. Wachau, S. Zhukov, J. Glaum, T. Granzow, H. von Seggern, and A. Klein, J. Appl. Phys. **108**, 104106 (2010).